Current Sharing Analysis of Three-Phase Interleaved *LLC* and Optimization Method to Reduce the Influence of Stray Inductance

Jiajia Guan, Jin Wen, *Graduate Student Member, IEEE*, Shuangxi Zhu, *Graduate Student Member, IEEE*, Zongheng Wu, Cai Chen, *Member, IEEE*, and Yong Kang, *Fellow, IEEE*

***Abstract*—Three-phase interleaved *LLC* is widely used because it can increase power capacity and reduce output current ripple. However, this article found that the three-phase interleaved *LLC* with all the resonant components using the delta connection (full-Δ type) has poor current-sharing characteristics. This article establishes the current sharing analysis model of three-phase interleaved *LLC*, explains the reasons for its poor current sharing effect, and proposes that changing the resonant capacitor to Y-type (Δ-Cr-Y type) can improve the current sharing effect. Further, to reduce the influence of stray inductance asymmetry on the current sharing, taking the Δ-Cr-Y type as an example, this article deduces the equivalent circuit model including stray inductance and proposes a current sharing optimization method without additional components. The proposed method can obtain the stray inductance of the three-phase resonant tank. Based on the stray inductance, the resonant inductance can be adjusted to obtain a better current-sharing effect. Finally, the proposed model and optimization method are verified by simulation and experiments. Compared with the full-Δ type, the proposed Δ-Cr-Y type shows higher current balance performance, and the proposed optimization method can further reduce the line current unbalance factor by more than 85%, and the phase current unbalance factor by more than 60%.**

***Index Terms*—Current imbalance, current sharing optimization, stray inductance, three-phase interleaved *LLC*.**

I. Introduction

LLC is a widely used topology for primary and secondary side isolation [1], [2], [3], [4], [5], [6]. To increase the power capacity, multiphase interleaved paralleling is a feasible method. Among them, the three-phase interleaved *LLC* converter has gained significant research attention. Many articles have analyzed the output current ripple characteristics of the multiphase interleaved *LLC* converter, as well as the working principle of three-phase interleaved *LLC* converter [7], [8], [9], [10], [11], [12], [13], [14], [15], [16]. In addition to increasing the power capacity of the system, the three-phase interleaved *LLC* converter can achieve a more balanced loss distribution, reduce the output current ripple, reduce the volume of the filter capacitor, and decrease the capacitor loss [17]. However, these advantages are greatly reduced when the currents of the three phases are imbalanced.

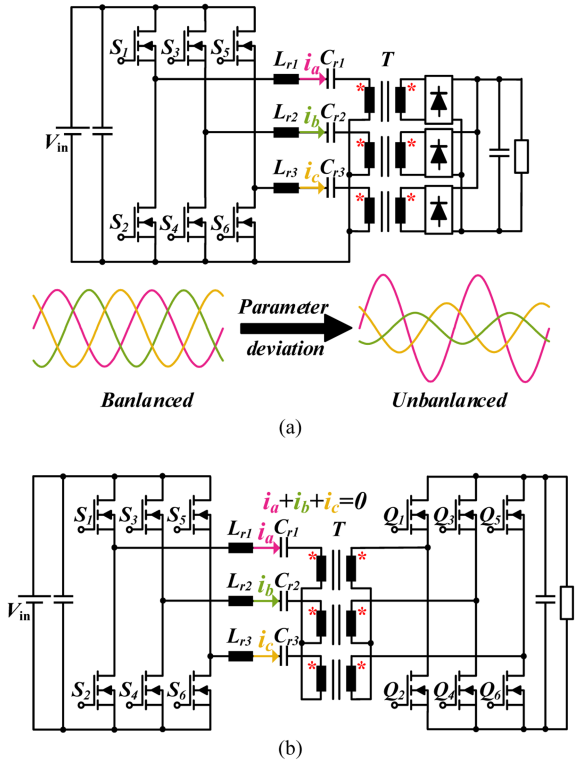

Fig. 1. Two topologies of three-phase interleaved *LLC*. (a) Traditional three-phase direct interleaved parallel *LLC*. (b) Three-phase interleaved *LLC* topology with transformer star connection.

As shown in Fig. 1(a), even a slight deviation in the device parameters of each phase can result in a significant current imbalance in the traditional three-phase direct interleaved parallel *LLC* converter. Therefore, various current balancing methods have been proposed in existing papers. Based on the first harmonic equivalent circuit, Arshadi et al. [17], [18] concluded that the deviation of the resonant inductance and the resonant capacitor has the same influence on the current sharing and is greater than

Manuscript received 9 June 2023; revised 31 July 2023, 12 October 2023, and 20 November 2023; accepted 7 December 2023. Date of publication 12 December 2023; date of current version 26 January 2024. Recommended for publication by Associate Editor H. Iu. *(Corresponding author: Cai Chen.)*

The authors are with the Huazhong University of Science and Technology, Wuhan 430074, China (e-mail: jiajiaguan@hust.edu.cn; wenjin@hust.edu.cn; xi_zi@hust.edu.cn; d201780377@hust.edu.cn; caichen@hust.edu.cn; ykang@hust.edu.cn).

Color versions of one or more figures in this article are available at https://doi.org/10.1109/TPEL.2023.3342036.

Digital Object Identifier 10.1109/TPEL.2023.3342036

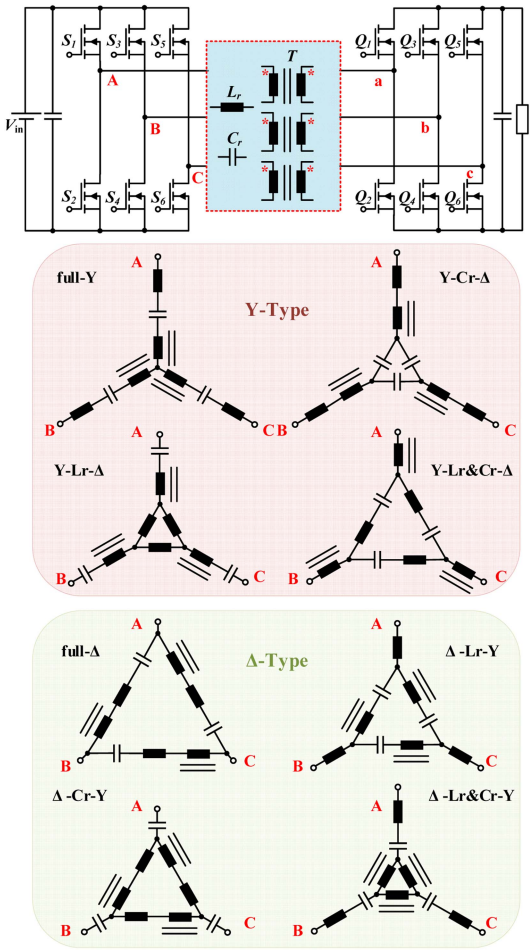

Fig. 2. Different connection structures of three-phase interleaved *LLC*.

the influence of the magnetizing inductance on the current sharing. The paper proposes to sample the resonant tank current and make the three-phase current more balanced by phase shifting. To enhance the current balance performance, Noah et al. [19], [20] introduced a balancing transformer with three windings into the primary circuit, which ensures that the vector sum of the three-phase currents is zero and results in a good current balance effect. In the application of ac to dc, Kim et al. [21], [22] added three power factor correction (PFC) circuits in the front stage of the three-phase interleaved *LLC*, and made the current balance by adjusting the output voltage of the PFC stage. Some studies have utilized switch-controlled inductors or capacitors to adjust the parameters of the resonant element and optimize the current balance performance [23], [24], [25]. However, if the above-mentioned active control method is used to improve the current-sharing characteristics, additional components will be introduced to increase the cost and complexity of the system. In addition to active control, many articles use resonant tank Y-connected type three-phase interleaved *LLC* to improve the current-sharing characteristics of the system, as shown in Fig. 1(b) [10], [11], [12]. Further, to reduce the transformer loss, some papers use the Δ-type three-phase interleaved *LLC* with the resonant tank changed to Δ-type connection (see Fig. 2) [26], [27].

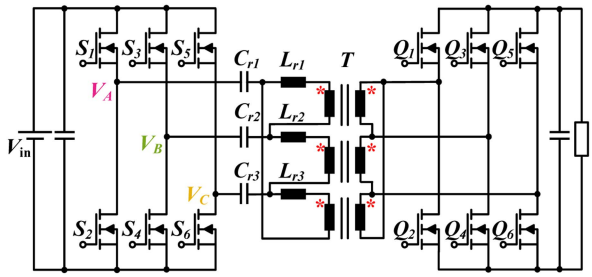

Fig. 3. Topology of the Δ-Cr-Y three-phase interleaved *LLC*.

However, this article found that the different connection methods of the resonant tank not only affect the loss, but also affect the current-sharing characteristics. To analyze the differences in the current-sharing characteristic of different three-phase interleaved *LLC* topologies and guide the topology selection, this article first proposes to use the three-power parallel model to analyze the current-sharing characteristic of three-phase interleaved *LLC*. Based on the proposed model, this article compares the difference in current-sharing characteristics between the full-Y type and the full-Δ type. It is theoretically concluded that the current-sharing characteristic of the full-Δ type three-phase interleaved *LLC* is poor. Further, this article proposes the topology of changing the resonant capacitor to Y-connection (Δ-Cr-Y type) or changing the resonant inductance to Y-connection (Δ-Lr-Y type). This not only improves the current-sharing characteristic of the full-Δ type, but also has the same transformer losses. Taking Δ-Cr-Y type (see Fig. 3) as an example, this article analyzed the principle that it can improve the current-sharing characteristic. In addition, this article gives the difference in current-sharing characteristics of different three-phase interleaved *LLC* topologies, which can provide a reference for the selection of three-phase interleaved *LLC* topology.

According to the analysis in this article, some three-phase interleaved *LLC* topologies can improve the current-sharing characteristic. Within the error range of the resonant capacitance, the current sharing effect has little change. However, when the deviation of the resonant inductance becomes larger, the effect of current sharing becomes worse. Due to the particularity of the three-phase interleaved *LLC* topology, it is difficult to ensure that the structure of each phase is completely symmetrical when making a prototype. This results in different line inductance and transformer leakage inductance for each phase and exacerbates the current imbalance. The simplest method to reduce the effect of stray inductance is to adjust the resonant inductance of each phase to compensate for the difference in stray inductance. However, there are two problems: 1) the actual line inductance and transformer leakage inductance are difficult to measure; 2) due to the mutual coupling of the three-phase circuits, it is impossible to balance the three-phase circuits by adjusting the resonant inductance of a certain phase.

To solve the above problems, taking the Δ-Cr-Y type three-phase interleaved *LLC* as an example, this article deduces the first harmonic equivalent model of the three-phase interleaved *LLC* including stray inductance. Based on this model, this article

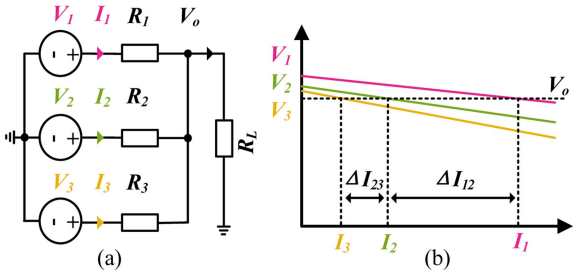

Fig. 4. Parallel model of three-phase voltage sources. (a) Circuit model. (b) Output characteristic curve.

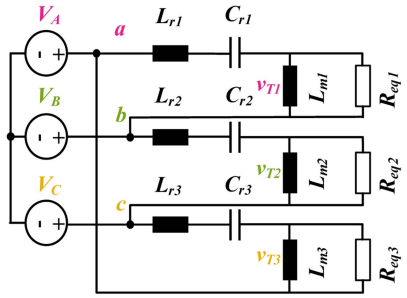

Fig. 5. Equivalent circuit of full Δ-type three-phase interleaved *LLC*.

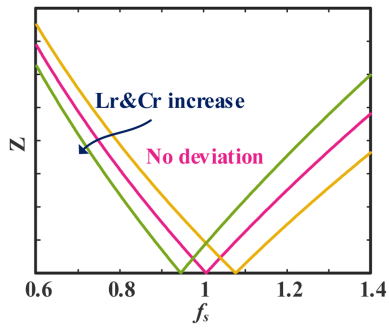

Fig. 6. Impedance of resonant tank.

proposes an optimization method that can reduce the influence of stray inductance without additional components. The proposed optimization method can obtain the sum of the equivalent line inductance and transformer leakage inductance of each phase. Combined with the proposed circuit model including stray inductance, the three-phase resonant inductance can be adjusted simultaneously to reduce the influence of stray inductance.

The rest of this article is organized as follows. Section II establishes the three-phase interleaved *LLC* parallel analysis model and explains the reason for the poor current sharing performance of the full-Δ type. This section proposed that changing the resonant capacitor to Y-type can improve the current sharing performance of the full-Δ type, and it is verified by simulation. Section III establishes an equivalent circuit model including stray inductance and proposes an optimization method that can reduce the influence of stray inductance on current sharing without additional components. Section IV provides the experimental results of a 2-kW prototype, which verifies the result of the theoretical analysis of the previous two sections. Finally, Section V concludes this article.

II. Analysis and Improvement of Δ-Type Three-Phase Interleaved *LLC* Current-Sharing Characteristics

A. Parallel Model of Three Voltage Sources and Analysis of Current-Sharing Characteristic of Full-Δ Type

Both Y-type and Δ-type three-phase interleaved *LLC* can be equivalent to the three-phase parallel power supply with coupling. Therefore, to analyze its current-sharing characteristic, the basic three-phase voltage source parallel model can be established first. It should be noted that due to the lack of an accurate gain model, the model proposed in this section is an analytical model, which is only used to qualitatively compare the current-sharing characteristics of different topologies. As shown in Fig. 4, $V_1/V_2/V_3$ is the ideal voltage source, $R_1/R_2/R_3$ is the output resistance of the power supply, and the output current deviation between the two phases can be obtained according to Kirchhoff's law (1), (2). It can be seen that only the difference in the no-load voltage or the difference in the output resistance has a great influence on the current-sharing effect of the three-phase circuit. To achieve a better current-sharing effect, the no-load voltage deviation and output resistance deviation should be minimized. In addition, increasing the output resistance can also reduce ΔI. However, simply increasing the output resistance will affect the output characteristic of the power supply

$$\begin{cases} V_o = V_1 - I_1 R_1 \\ V_o = V_2 - I_2 R_2 \\ V_o = V_3 - I_3 R_3 \end{cases} \tag{1}$$

$$\begin{cases} \Delta I_{12} = I_1 - I_2 = \frac{R_2 V_1 - R_1 V_2 + V_o(R_1 - R_2)}{R_1 R_2} \\ \Delta I_{23} = I_2 - I_3 = \frac{R_3 V_2 - R_2 V_3 + V_o(R_2 - R_3)}{R_2 R_3} \end{cases}. \tag{2}$$

To better analyze the current-sharing characteristic and facilitate comparison, (3) defines the current unbalance factor (U_f) [17]. The numerator is related to the loss difference between the phase with the largest current and the phase with the smallest current, and the denominator is related to the total loss

$$U_{\mathrm{f}} = \frac{\mathrm{Max}\left(I_{\mathrm{a}}^2, I_{\mathrm{b}}^2, I_{\mathrm{c}}^2\right) - \mathrm{Min}\left(I_{\mathrm{a}}^2, I_{\mathrm{b}}^2, I_{\mathrm{c}}^2\right)}{I_{\mathrm{a}}^2 + I_{\mathrm{b}}^2 + I_{\mathrm{c}}^2} \tag{3}$$

where I_a, I_b, and I_c are the line current.

The equivalent circuit of the full-Δ type three-phase interleaved *LLC* is shown in Fig. 5. $V_A/V_B/V_C$ is the three-phase voltage source equivalent to the input voltage source and the three-phase half-bridge. When the parameters of the resonant element deviate, the impedance variation of the resonant tank can be obtained (see Fig. 6). Due to the clamping effect of the output capacitor, the RMS value of the transformer primary voltages ($v_{T1}/v_{T2}/v_{T3}$) are the same. Taking phase A as an example, its phase current can be obtained according to Kirchhoff's law (4). It can be seen that there is no coupling in the three-phase output circuit, and the current of each phase is only related to the voltage at both ends of the resonant tank (V_{ab}) and the impedance of the

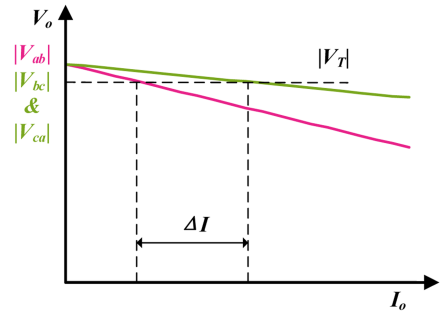

Fig. 7. Full Δ-type three-phase interleaved *LLC* output characteristic curve.

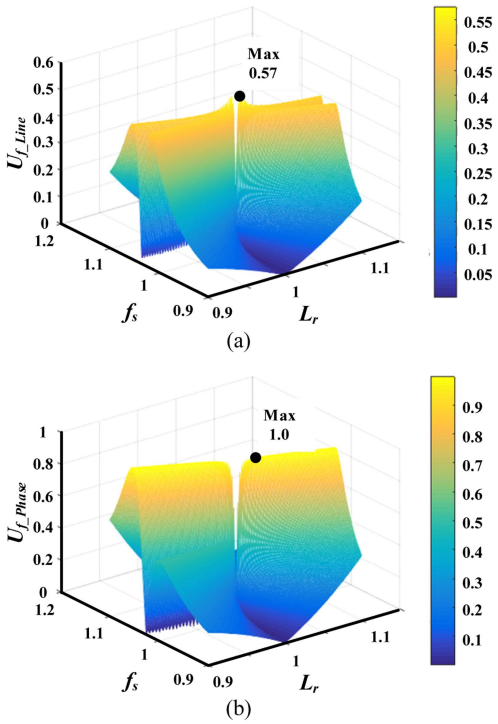

Fig. 8. U_f variation of full-Δ type three-phase interleaved *LLC*. (a) Line current. (b) Phase current.

resonant tank

$$\begin{cases} V_{ab} = V_A - V_B \\ I_{ab} = \frac{V_{ab} - v_{T1}}{j\omega L_{r1} + 1/(j\omega C_{r1})} \end{cases}. \tag{4}$$

Considering that the resonant inductance of phase A is less than the rated value, and there is no deviation between phase B and phase C, it can be seen from Fig. 6 that when the switching frequency is near the resonant frequency, the impedance of the resonant tanks of each phase is small and the difference is large. The RMS values of the three-phase equivalent input voltages (V_{ab}/V_{bc}/V_{ca}) are equal, but the output impedances differ greatly, so the output characteristic curve of the three-phase power supply can be obtained (see Fig. 7). It can be seen that there will be a large imbalance in the phase current (I_{ab}/I_{bc}/I_{ca}).

Furthe, Fig. 8 shows the change of line current U_f and phase current U_f of the full-Δ type three-phase interleaved *LLC* when

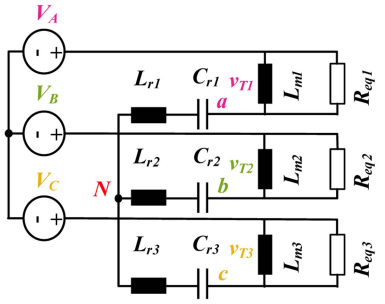

Fig. 9. Equivalent circuit of full Y-type three-phase interleaved *LLC*.

the switching frequency and the resonant inductance of phase A changed (3) and (4). When the resonant inductance has no deviation, the three-phase current is balanced, so U_f is equal to 0. When there is a deviation in the resonant inductance, as shown in Fig. 8(a), the maximum line current U_f is about 0.57, which means that the line current of full-Δ type still has a good sharing effect. However, as shown in Fig. 8(b), the maximum phase current U_f is 1, which means that when the resonance parameter deviates, a certain phase transmits all the power, and the current is seriously unbalanced. This is consistent with the conclusion based on the analysis of the output characteristic curve. Therefore, although the full-Δ type three-phase interleaved *LLC* has lower transformer losses, its current-sharing characteristic is poor.

B. Analysis of Current-Sharing Characteristic of Full-Y Type

The equivalent circuit of the full-Y type three-phase interleaved *LLC* is shown in Fig. 9. V_A/V_B/V_C is the three-phase voltage source equivalent to the input voltage source and the three-phase half-bridge. Due to the clamping effect of the output capacitor, the RMS value of the transformer primary voltages (v_{T1}/v_{T2}/v_{T3}) are the same. According to Kirchhoff's law, the impedance of the resonant tank (Z_{aN}/Z_{bN}/Z_{cN}) and the equivalent input voltage (V_{AN}/V_{BN}/V_{CN}) of the three-phase circuit can be obtained (5)–(9). It can be seen that the three-phase circuits are coupled to each other, and when the impedance changes, V_{AN}/V_{BN}/V_{CN} will change

$$\begin{cases} Z_{aN} = j\omega L_{r1} + 1/(j\omega C_{r1}) \\ Z_{bN} = j\omega L_{r2} + 1/(j\omega C_{r2}) \\ Z_{cN} = j\omega L_{r3} + 1/(j\omega C_{r3}) \end{cases} \tag{5}$$

$$\begin{cases} V_{AN} = V_A - V_N \\ V_{BN} = V_B - V_N \\ V_{CN} = V_C - V_N \end{cases} \tag{6}$$

$$\begin{cases} I_a + I_b + I_c = 0 \\ I_a = (V_{AN} - v_{T1})/Z_{aN} \\ I_b = (V_{BN} - v_{T2})/Z_{bN} \\ I_c = (V_{CN} - v_{T3})/Z_{cN} \end{cases} \tag{7}$$

$$\begin{cases} V_{AN} = \frac{Z_{aN}Z_{cN}(V_A - V_B) + Z_{aN}Z_{bN}(V_A - V_C) - V_S}{Z_{aN}Z_{bN} + Z_{bN}Z_{cN} + Z_{aN}Z_{cN}} \\ V_{BN} = \frac{Z_{aN}Z_{bN}(V_B - V_C) + Z_{bN}Z_{cN}(V_B - V_A) - V_S}{Z_{aN}Z_{bN} + Z_{bN}Z_{cN} + Z_{aN}Z_{cN}} \\ V_{CN} = \frac{Z_{bN}Z_{cN}(V_C - V_A) + Z_{aN}Z_{cN}(V_C - V_B) - V_S}{Z_{aN}Z_{bN} + Z_{bN}Z_{cN} + Z_{aN}Z_{cN}} \end{cases} \tag{8}$$

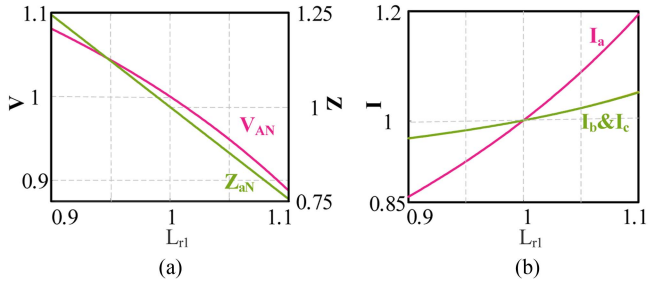

Fig. 10. Changes in impedance and current when the resonant inductance of phase A is different. (a) Impedance and input voltage of phase A. (b) Three-phase line current.

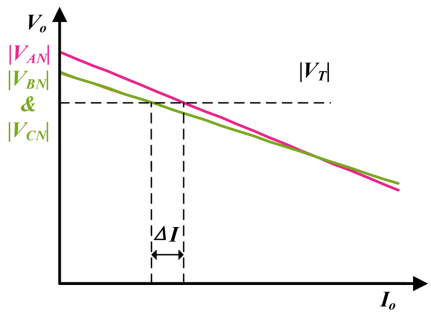

Fig. 11. Full Y-type three-phase interleaved *LLC* output characteristic curve.

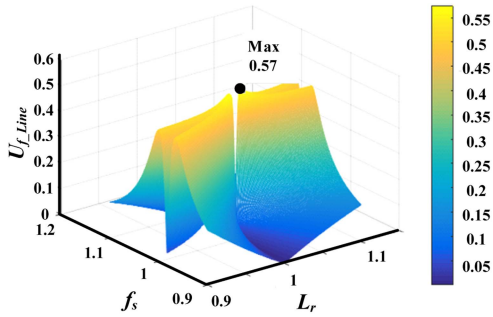

Fig. 12. U_f variation of full Y-type three-phase interleaved *LLC*.

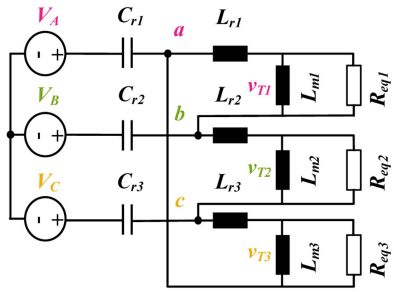

Fig. 13. Equivalent circuit of Δ-Cr-Y type three-phase interleaved *LLC*.

where

$$V_S = -Z_{aN}Z_{bN}V_{T3} - Z_{bN}Z_{cN}V_{T1} - Z_{aN}Z_{cN}V_{T2}. \quad (9)$$

When the switching frequency is lower than the resonant frequency, taking phase A as example, Fig. 10(a) shows the normalized changes in the equivalent input voltage and impedance of phase A when the resonant inductance changes. It can be seen that as the inductance decreases, its impedance increases. However, its input voltage (V_{AN}) will also increase, and the changing trend of the voltage and impedance is the same, which can suppress the current change of phase A. Fig. 10(b) is the change of three-phase current, and Fig. 11 is the output characteristic curve of the three-phase power supply when the resonant inductance is deviated. It can be seen that when the resonant inductance has deviation, the change of the equivalent input voltage can suppress the unbalance of the three-phase current. The same conclusion can also be obtained when the switching frequency is greater than the resonant frequency.

Further, Fig. 12 shows the change of the line current U_f of the full-Y type three-phase interleaved *LLC* when the switching frequency and the resonant inductance of phase A changed. When the resonant inductance has no deviation, the three-phase current is balanced, so U_f is equal to 0. When the inductance has a deviation, the maximum U_f is about 0.57. This means that when the resonance parameter deviates, the full-Y type three-phase interleaved *LLC* will not transmit all the power in one phase. Therefore, the full-Y type three-phase interleaved *LLC* can improve the current-sharing characteristic.

From the above analysis, it can be concluded that when the resonance parameter deviates, the full-Y type three-phase interleaved *LLC* will automatically adjust the equivalent input voltage of the three-phase circuit, reduce the unbalance of the three-phase current, and improve the current-sharing characteristic.

C. Analysis of Current-Sharing Characteristic of Δ-Cr-Y Type

According to the previous analysis, although the full-Δ type has higher efficiency, its current-sharing characteristic is poor. Compared with the full-Δ type, the full-Y type has higher transformer loss, but its current-sharing characteristic is better. Figs. 8(a) and 12 show that the line currents of the two topologies have good current-sharing characteristics. The main reason for the poor phase current-sharing characteristic of the full-Δ type is that there is no coupling in the equivalent output impedance of the three-phase power supply, and the output impedance changes greatly when the resonance parameters deviate. To combine the advantages of the two topologies and improve the current sharing performance of the full-Δ type, this article proposes to change the resonant capacitor to Y-type connection (Δ-Cr-Y type) or the resonant inductance to Y-type connection (Δ-Lr-Y type). Taking the Δ-Cr-Y type as an example, based on the proposed three-power analysis model, the principle of improving current sharing performance will be analyzed below.

The equivalent circuit of Δ-Cr-Y type three-phase interleaved *LLC* is shown in Fig. 13, and the three-phase equivalent input power ($V_{ab}/V_{bc}/V_{ca}$) can be obtained (10) and (11). According to Kirchhoff's law, the three-phase line current and phase current can be obtained (12). It can be seen that the output impedances of the three-phase power supplies are coupled to each other, and changes in impedance will cause changes in $V_{ab}/V_{bc}/V_{ca}$.

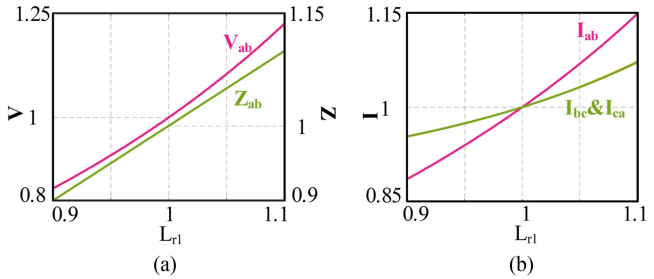

Fig. 14. Changes in impedance and current when the resonant inductance of phase ab is different. (a) Impedance and input voltage of phase ab. (b) Three-phase current.

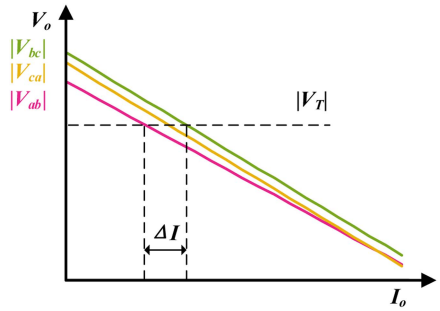

Fig. 15. Δ-Cr-Y type three-phase interleaved *LLC* output characteristic curve.

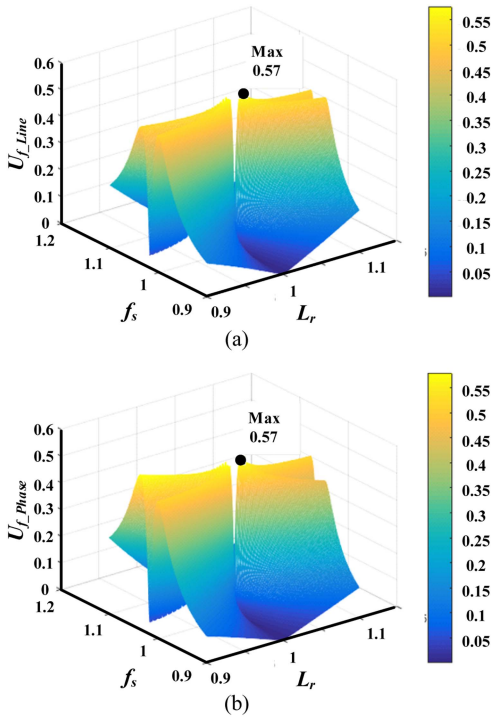

Fig. 16. U_f variation of Δ-Cr-Y type three-phase interleaved *LLC*. (a) Line current. (b) Phase current.

Based on the previous analysis, it can be seen that no matter which connection method is adopted for the resonant elements, the three-phase line current ($I_a/I_b/I_c$) has better current-sharing characteristic, so the following mainly analyzes the changes of the phase current

$$\begin{cases} V_{ab} = V_A - V_B - i_a Z_{Cr1} + i_b Z_{Cr2} \\ V_{bc} = V_B - V_C - i_b Z_{Cr2} + i_c Z_{Cr3} \\ V_{ca} = V_C - V_A - i_c Z_{Cr3} + i_a Z_{Cr1} \end{cases} \tag{10}$$

$$\begin{cases} Z_{Lrn,n=1,2,3} = j\omega L_{rn,n=1,2,3} \\ Z_{Crn,n=1,2,3} = 1/(j\omega C_{rn,n=1,2,3}) \end{cases} \tag{11}$$

$$\begin{cases} I_{ab} = (V_{ab} - v_{T1})/Z_{Lr1} \\ I_{bc} = (V_{bc} - v_{T2})/Z_{Lr2} \\ I_{ca} = (V_{ca} - v_{T3})/Z_{Lr3} \\ I_a = I_{ab} - I_{ca} \\ I_b = I_{bc} - I_{ab} \\ I_c = I_{ca} - I_{bc} \end{cases}. \tag{12}$$

When the switching frequency is lower than the resonant frequency, taking phase-ab as an example, Fig. 14(a) shows the normalized voltage and impedance changes of phase-ab when there is a deviation in the resonant inductance. It can be seen that when the inductance decreases, its impedance decreases. However, its input voltage (V_{ab}) will also decrease, and the changing trend of the voltage and impedance are the same, which can suppress the current change of phase-ab. Fig. 14(b) shows the change of the three-phase current, and Fig. 15 shows the output characteristic curve of the three-phase power supply when the resonant inductance deviates. It can be seen that when the resonant inductance has deviation, the change of the equivalent input voltage can suppress the unbalance of the three-phase current. The same conclusion can also be obtained when the switching frequency is greater than the resonant frequency.

Further, Fig. 16 shows the change of the Δ-Cr-Y type three-phase interleaved *LLC* line current and phase current unbalanced factor when the switching frequency and the resonant inductance of the phase-ab are changed. It can be seen that the maximum U_f of the line current and phase current of the Δ-Cr-Y type are the same as that of the full-Y type, both of which are about 0.57. This means that there is no case where one phase transmits all the power as in the full-Δ type.

Therefore, by changing the resonant capacitor to Y-type connection, the current sharing performance of the full-Δ type can be improved. Meanwhile, it has the same low transformer loss characteristic as the full-Δ type. Based on the same analysis method, it is easy to know that the Δ-Lr-Y type and Δ-Lr&Cr-Y type three-phase interleaved *LLC* can also improve the current-sharing characteristics.

D. Circuit Simulation Verification

This section verifies the previous analysis through simulation. Table I shows the simulation parameters of full-Y type three-phase interleaved *LLC*, and the parameters of other types of topologies can be obtained through star-delta transformation. When considering the inherent deviation of resonant inductance and resonant capacitor, generally consider a 5% deviation for NP0 material capacitor, and 10% deviation for resonant inductance [28].

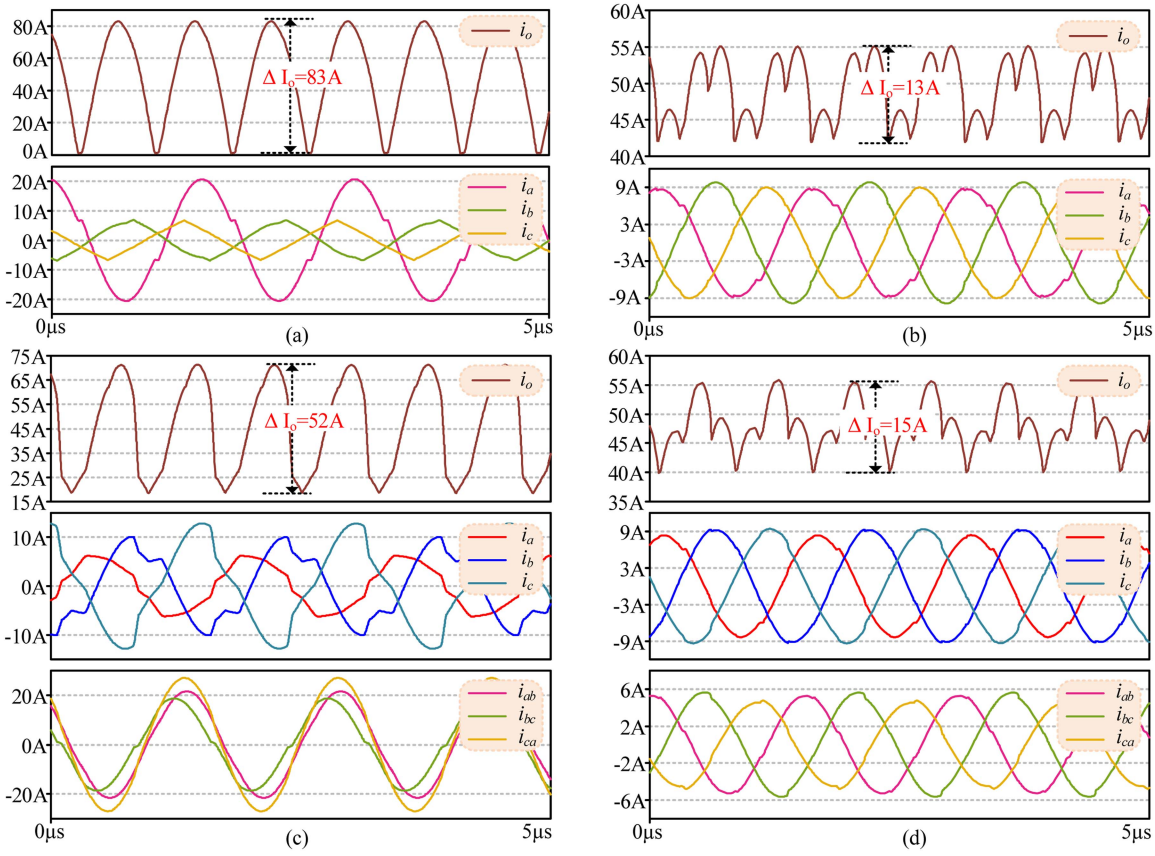

Fig. 17. Simulation results of four topologies in case I. (a) Direct interleaved parallel type. (b) Full-Y type. (c) Full-Δ type. (d) Δ-Cr-Y type.

TABLE I
CIRCUIT PARAMETERS OF THE SIMULATION

Parameters	Value
V_i	400 V
V_o	48 V
f_r	650 kHz
L_m	11 μH
L_r	2.2 μH ± 10%
C_r	27 nF ± 5%

TABLE II
DIFFERENT IMPEDANCE CASES FOR SIMULATION

Case	Phase A	Phase B	Phase C
	L_{r1}, C_{r1}	L_{r2}, C_{r2}	L_{r3}, C_{r3}
Case I	1.98 μH, 27 nF	2.2 μH, 27 nF	2.42 μH, 27 nF
Case II	2.2 μH, 29.7 nF	2.2 μH, 27 nF	2.2 μH, 24.3 nF

To fully consider the impact of the inconsistency of the three-phase parameters and facilitate comparison, this article designs the simulation parameters shown in Table II. Case I is that the resonant inductance has deviation, and the resonant capacitor has no deviation. Case II is that the resonant capacitor has deviation, and the resonant inductance has no deviation. In both cases, the parameter of one phase is less than the rated parameter, the parameter of one phase has no deviation, and the parameter of one phase is greater than the rated parameter. The normalized frequencies for all simulations are consistent and are resonant frequencies.

Fig. 17 shows the current waveforms of four types of three-phase interleaved *LLC* in Case I. As shown in Fig. 17(a), the three-phase current of the direct parallel type is completely unbalanced, and only phase A transmits power. The current of phase B and phase C is equal to the magnetizing current, and no power is transmitted to the secondary side. The three-phase current of the full-Δ type is also unbalanced, and there is a large circulating current in the phase current. In contrast, the other two three-phase interleaved *LLC* topologies (full-Y type and Δ-Cr-Y type) both have better current-sharing characteristics.

Fig. 18 shows the current waveforms of four types of three-phase interleaved *LLC* in Case II. As shown in Fig. 18(a), the three-phase current of the direct parallel type is completely unbalanced, and only phase C transmits power. The current of phase A and phase B is equal to the magnetizing current, and no power is transmitted to the secondary side. The three-phase current of the full-Δ type is also unbalanced, and there is a large circulating current in the phase current. In contrast, the other two three-phase interleaved *LLC* topologies (full-Y type and Δ-Cr-Y type) both have better current-sharing characteristics.

Therefore, both the direct parallel type and the full-Δ type have large current unbalance problems, and additional current

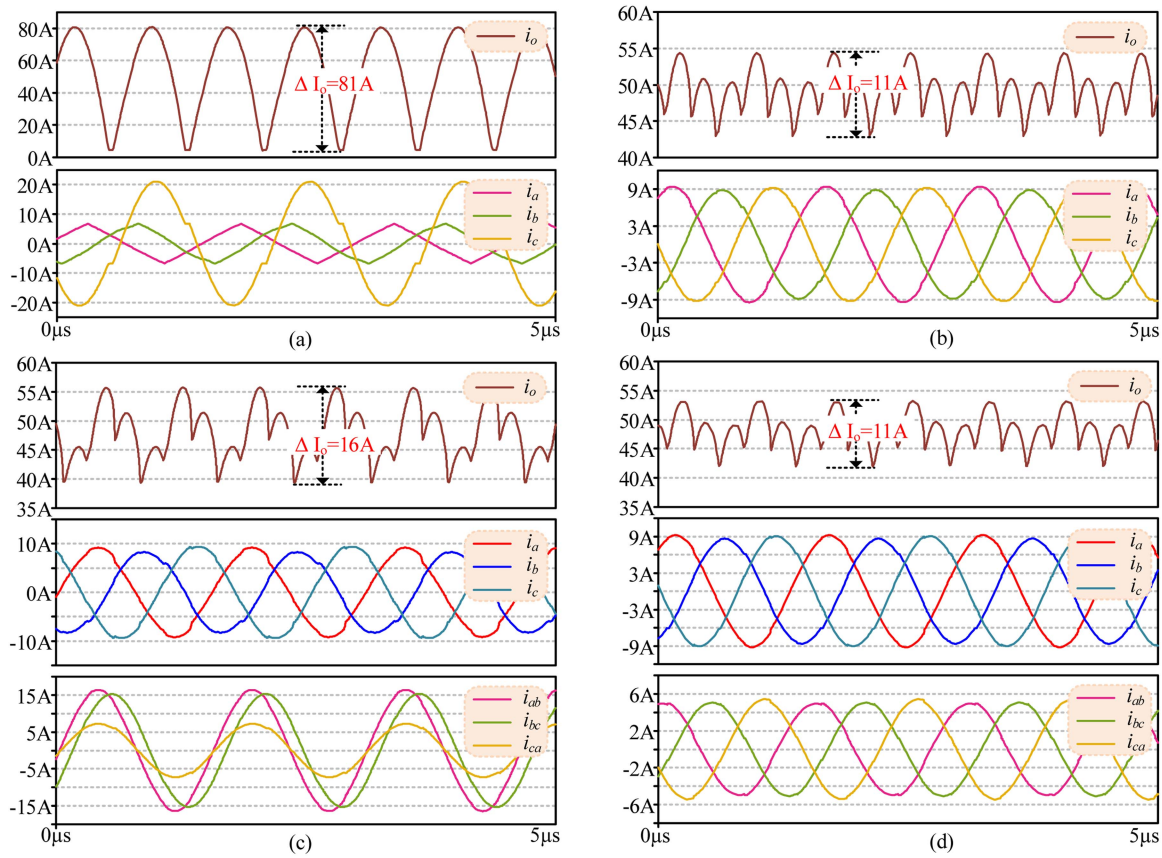

Fig. 18. Simulation results of four topologies in case II. (a) Direct interleaved parallel type. (b) Full-Y type. (c) Full-Δ type. (d) Δ-Cr-Y type.

TABLE III
COMPARISON OF ICS EFFECTS OF DIFFERENT TOPOLOGIES

Topology	ICS	Max. U_f
Full-Y	√	0.57
Y-Cr-Δ	√	0.57
Y-Lr-Δ	√	0.57
Y-Cr&Lr-Δ	×	1.0
Full-Δ	×	1.0
Δ-Cr-Y	√	0.57
Δ-Lr-Y	√	0.57
Δ-Cr&Lr-Y	√	0.57

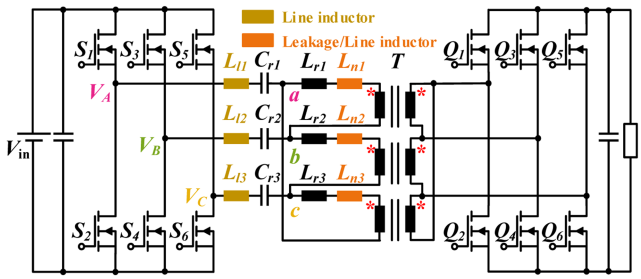

Fig. 19. Δ-Cr-Y type three-phase interleaved *LLC* including stray inductance.

sharing measures need to be taken in practical applications, which will increase the cost and complexity of the system. It can be seen that the simulation results are consistent with the previous theoretical analysis results, and the current balance performance of the full-Δ type three-phase interleaved *LLC* can be improved by changing the connection form of the resonant inductor or resonant capacitor. Based on the same analysis method, the improved current sharing (ICS) effects of different three-phase interleaved *LLC* topologies in Fig. 2 can be obtained, as shown in Table III, which can guide the selection of three-phase interleaved *LLC* topologies. It can be seen that once both the resonant inductor and the resonant capacitor are connected in delta-type, the current-sharing characteristic of the topology will be poor.

III. CURRENT SHARING OPTIMIZATION METHOD TO REDUCE THE INFLUENCE OF STRAY INDUCTANCE

According to the analysis of Section II, the Δ-Cr-Y type can improve the current balance effect of the full-Δ type. As shown in Figs. 17(d) and 18(d), within the considered deviation range, the resonant inductance and resonant capacitance have little influence on the current sharing effect of the Δ-Cr-Y type three-phase interleaved *LLC*. However, due to the particularity of the three-phase interleaved *LLC* topology, it is difficult to ensure that the structure of each phase is completely symmetrical when making a prototype (see Fig. 19). This results in different line inductance and transformer leakage inductance for each phase and exacerbates the current imbalance. The

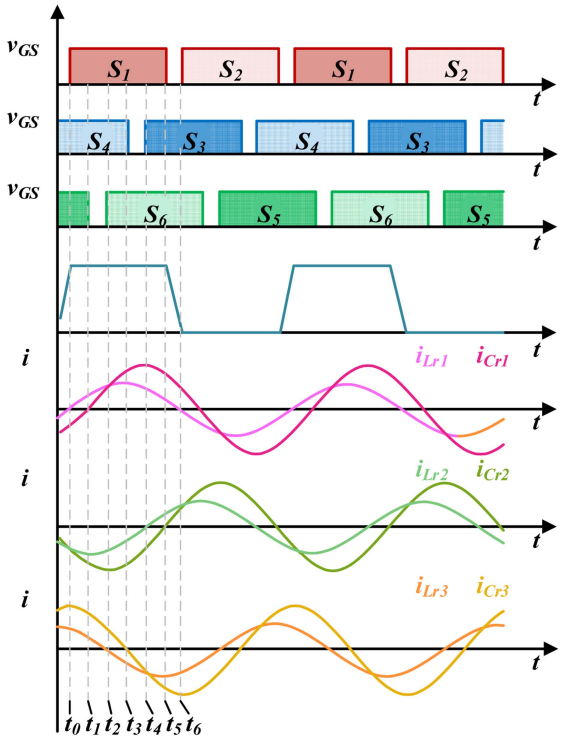

Fig. 20. Key waveforms of Δ-Cr-Y type three-phase interleaved *LLC*.

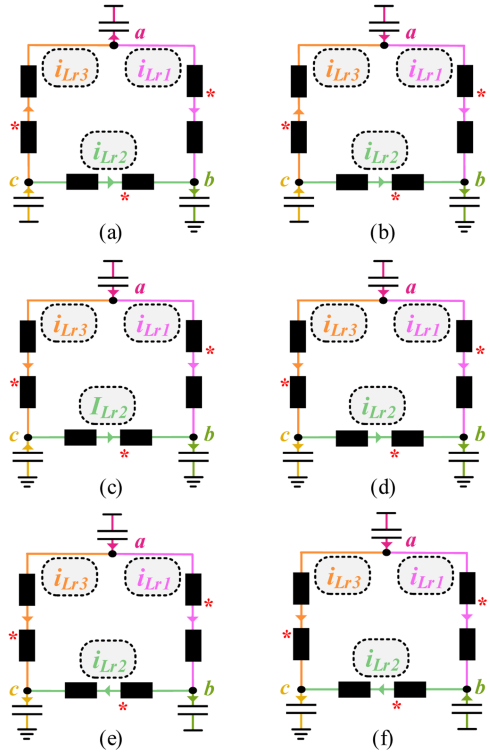

Fig. 21. Six equivalent circuits of resonant tank. (a) Mode I [t_0–t_1]: S_1, S_4, and S_5 are turned on and i_{Lr1} is greater than zero. (b) Mode II [t_1–t_2]: S_1 and S_4 are turned on and i_{cr1} is greater than zero. (c) Mode III [t_2–t_3]: S_1, S_4, and S_6 are turned on and i_{Lr3} is less than zero. (d) Mode IV [t_3–t_4]: S_1 and S_6 are turned on and i_{Cr3} is less than zero. (e) Mode V [t_4–t_5]: S_1, S_4, and S_6 are turned on and i_{Lr2} is great than zero. (f) Mode VI [t_5–t_6]: S_3 and S_6 are turned on and i_{Cr2} is greater than zero.

simplest method to reduce the effect of stray inductance is to adjust the resonant inductance of each phase to compensate for the difference in stray inductance. However, there are two problems: 1) the actual line inductance and transformer leakage inductance are difficult to measure; 2) due to the mutual coupling of the three-phase circuits, it is impossible to balance the three-phase circuits by adjusting the resonant inductance of a certain phase.

To solve the above problems, taking the Δ-Cr-Y type three-phase interleaved *LLC* as an example, this article deduces the equivalent circuit model of the three-phase interleaved *LLC* including stray inductance. Based on this model, this article proposes an optimization method that can reduce the influence of stray inductance without additional components.

A. *Resonant Mode Analysis of the Δ-Cr-Y Type Three-phase Interleaved* LLC

When the switching frequency is equal to the resonant frequency, the main working waveform of Δ-Cr-Y type three-phase interleaved *LLC* is shown in Fig. 20. The phases of the driving signals of the three half-bridges on the primary side are 120° from each other, and the driving signals on the secondary side are the same as those of the primary side. The phase of i_{Lr} is 30° ahead of i_{Cr}, and the amplitude of i_{Lr} is $1/\sqrt{3}$ of i_{Cr}. When the voltage drop of the switching device and the influence of the magnetizing current are ignored, the resonant tank has 12 working modes in one switching cycle. Taking S_1 turned on as an example, six modes are analyzed in this article, and the equivalent circuit is shown in Fig. 21. The other six working modes when S_1 is turned off are complementary to the six modes shown.

Mode I (t_0–t_1): S_1, S_4, and S_5 are turned ON, and i_{Lr1} is greater than zero. i_{Cr1} is equal to the difference between i_{Lr3} and i_{Lr1}; i_{Cr2} is equal to the sum of i_{Lr1} and i_{Lr2}; i_{Cr3} is equal to the sum of i_{Lr2} and i_{Lr3}.

Mode II (t_1–t_2): S_1 and S_4 are turned ON, i_{Cr1} is greater than zero. i_{Cr1} is equal to the difference between i_{Lr1} and i_{Lr3}; i_{Cr2} is equal to the sum of i_{Lr1} and i_{Lr2}; i_{Cr3} is equal to the sum of i_{Lr2} and i_{Lr3}.

Mode III (t_2–t_3): S_1, S_4, and S_6 are turned ON, i_{Lr3} is less than zero. i_{Cr1} is equal to the sum of i_{Lr1} and i_{Lr3}; i_{Cr2} is equal to the sum of i_{Lr1} and i_{Lr2}; i_{Cr3} is equal to the difference between i_{Lr2} and i_{Lr3}.

Mode IV (t_3–t_4): S_1 and S_6 are turned ON, i_{Cr3} is less than zero. i_{Cr1} is equal to the sum of i_{Lr1} and i_{Lr3}; i_{Cr2} is equal to the sum of i_{Lr1} and i_{Lr2}; i_{Cr3} is equal to the difference between i_{Lr3} and i_{Lr2}.

Mode V (t_4–t_5): S_1, S_4, and S_6 are turned ON, i_{Lr2} is greater than zero. i_{Cr1} is equal to the sum of i_{Lr1} and i_{Lr3}; i_{Cr2} is equal to the difference between i_{Lr1} and i_{Lr2}; i_{Cr3} is equal to the sum of i_{Lr2} and i_{Lr3}.

Mode VI (t_5–t_6): S_3 and S_6 are turned ON, i_{Cr2} is greater than zero. i_{Cr1} is equal to the sum of i_{Lr3} and i_{Lr1}; i_{Cr2} is equal

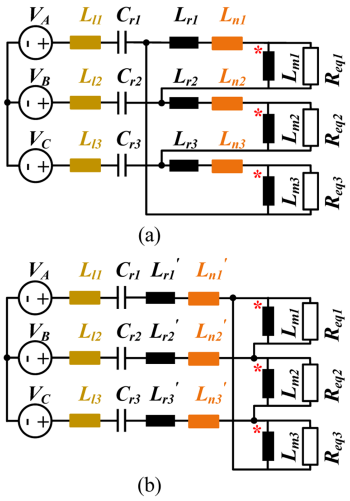

Fig. 22. Equivalent circuit of Δ-Cr-Y three-phase interleaved *LLC* with stray inductance. (a) Before star-delta transformation. (b) After star-delta transformation.

to the difference between i_{Lr2} and i_{Lr1}; i_{Cr3} is equal to the sum of i_{Lr2} and i_{Lr3}.

It can be seen that the resonant tanks of the Δ-Lr-Y three-phase interleaved *LLC* are coupled with each other. In a switching cycle, there is no fixed inductor to resonate with C_{r1}/ C_{r2}/ C_{r3}, and the resonant inductor is a virtual inductor obtained through transformation. When the stray inductors are unbalanced, it is difficult to achieve circuit balance by adjusting the resonant parameters of a certain phase.

B. Current Sharing Optimization Method to Reduce the Influence of Stray Inductance

Based on the previous analysis, a three-phase equivalent circuit including stray inductance can be obtained, as shown in Fig. 22(a). According to the star-delta transformation, the resonant inductance and leakage inductance can be changed into a Y-type connection, as shown in Fig. 22(b). The transformed resonant inductance $(L_{rn}{}',_{n=1,2,3})$ and line inductance $(L_{nn}{}',_{n=1,2,3})$ can be obtained according to the star-delta transformation (13) and (14). Therefore, the stray inductance ($L_{sn,n=}$ $_{1,2,3}$) of each phase is the sum of line inductance and leakage inductance (15). The equivalent resonant inductance (L_{ra}/L_{rb}/L_{rc}) of each phase is the sum of resonant inductance and stray inductance (16). According to (16), when the three-phase stray inductance is different, the value of the three-phase resonant inductance $(L'_{r1}/L'_{r2}/L'_{r3})$ can be adjusted to reduce the deviation of the three-phase equivalent resonant inductance (L_{ra}/L_{rb}/L_{rc}). However, this requires knowing the values of the three-phase stray inductances. The three-phase stray inductances are obtained by the equivalent transformation of the line inductance and leakage inductance, and it is difficult to measure the line inductance and leakage inductance accurately

$$\begin{cases} L'_{r1} = L_{r1}L_{r3}/(L_{r1}+L_{r2}+L_{r3}) \\ L'_{r2} = L_{r2}L_{r1}/(L_{r1}+L_{r2}+L_{r3}) \\ L'_{r3} = L_{r2}L_{r3}/(L_{r1}+L_{r2}+L_{r3}) \end{cases} \tag{13}$$

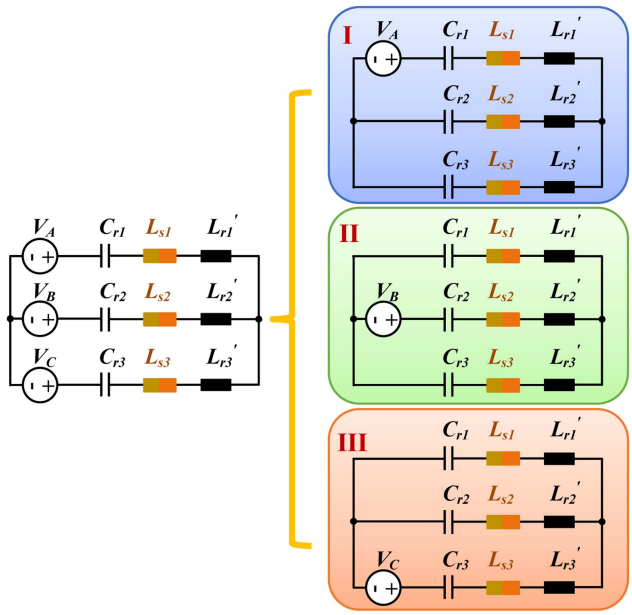

Fig. 23. Short-circuit equivalent circuit model after transformation.

$$\begin{cases} L'_{n1} = L_{n1}L_{n3}/(L_{n1}+L_{n2}+L_{n3}) \\ L'_{n2} = L_{n2}L_{n1}/(L_{n1}+L_{n2}+L_{n3}) \\ L'_{n3} = L_{n2}L_{n3}/(L_{n1}+L_{n2}+L_{n3}) \end{cases} \tag{14}$$

$$\begin{cases} L_{s1} = L'_{n1} + L_{l1} \\ L_{s2} = L'_{n2} + L_{l2} \\ L_{s3} = L'_{n3} + L_{l3} \end{cases} \tag{15}$$

$$\begin{cases} L_{ra} = L_{s1} + L'_{r1} \\ L_{rb} = L_{s2} + L'_{r2} \\ L_{rc} = L_{s3} + L'_{r3} \end{cases}. \tag{16}$$

To reduce the influence of stray inductance on current sharing and solve the problem that the line inductance and leakage inductance are difficult to measure, this article proposes to use the resonance method to measure three resonant frequencies respectively, and then the stray inductance of each phase can be obtained based on the calculation. It is not necessary to know the values of line inductance and leakage inductance for each phase. Combined with the equivalent model including stray inductance, the resonant inductance can be adjusted to make the three-phase current more balanced.

When the secondary side is short-circuited, the equivalent circuit model of the three-phase circuit is shown in Fig. 23. Combined with the short-circuit model, the proposed optimization process is shown in Fig. 24. The flow of the proposed optimization method is as follows.

Taking phase A as an example, when measuring the resonant frequency of phase A, the upper switches of phase B and phase C are kept OFF, and the lower switches are kept on. Therefore, the short-circuit model is the equivalent to circuit I. The equivalent resonant inductance (L_{rA}) and resonant capacitance (C_{rA}) can be calculated by (17). Whether the switching frequency is equal to the resonant frequency, (f_{nA}) can be judged according to the switching node voltage and current of phase A. If it is not at

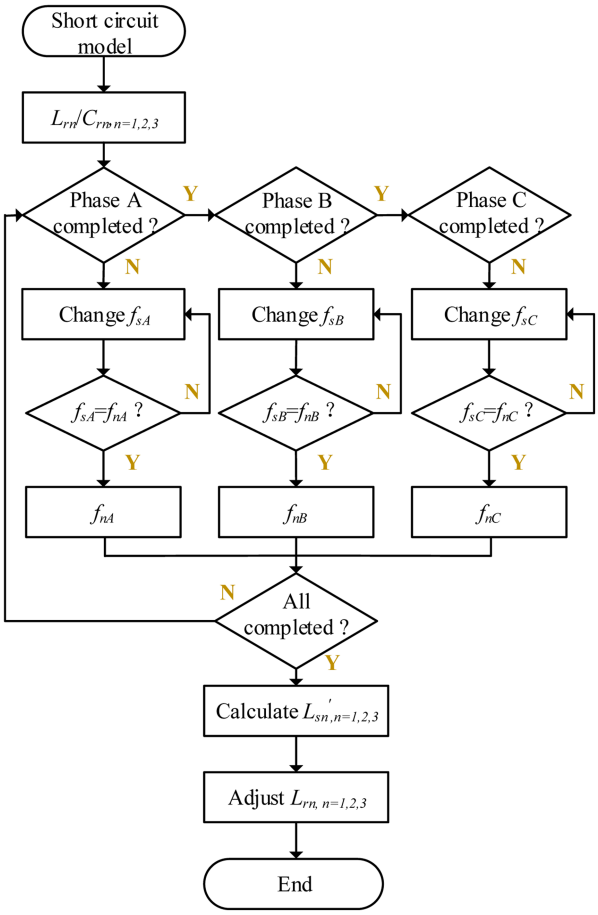

Fig. 24. Flowchart of the proposed optimization method.

the resonance point, modify the switching frequency until f_{sA} is equal to f_{nA}. Based on the same method, the resonant frequency of phase B and phase C and their equivalent resonant inductance and resonant capacitance can be obtained (18) and (19). Then, according to (17)–(19), the equivalent resonant inductance of each phase can be obtained (20). Further, the total stray inductance ($L_{sn,n=12,3}$) of each phase after star-delta transformation can be obtained according to (13), (16), (20)

$$\begin{cases} f_{nA} = 1/(2\pi\sqrt{L_{rA}C_{rA}}) \\ L_{rA} = L_{ra} + L_{rb}//L_{rc} \\ C_{rA} = C_{r1}(C_{r2}+C_{r3})/(C_{r1}+C_{r2}+C_{r3}) \end{cases} \tag{17}$$

$$\begin{cases} f_{nB} = 1/(2\pi\sqrt{L_{rB}C_{rB}}) \\ L_{rB} = L_{rb} + L_{ra}//L_{rc} \\ C_{rB} = C_{r2}(C_{r1}+C_{r3})/(C_{r1}+C_{r2}+C_{r3}) \end{cases} \tag{18}$$

$$\begin{cases} f_{nC} = 1/(2\pi\sqrt{L_{rC}C_{rC}}) \\ L_{rC} = L_{rc} + L_{ra}//L_{rb} \\ C_{rC} = C_{r3}(C_{r1}+C_{r2})/(C_{r1}+C_{r2}+C_{r3}) \end{cases} \tag{19}$$

$$\begin{cases} L_{ra} = \frac{2(C_{rA}\omega_{nA}^2 - C_{rB}\omega_{nB}^2 - C_{rC}\omega_{nC}^2)}{\text{Den}} \\ L_{rb} = \frac{2(-C_{rA}\omega_{nA}^2 + C_{rB}\omega_{nB}^2 - C_{rC}\omega_{nC}^2)}{\text{Den}} \\ L_{rc} = \frac{2(-C_{rA}\omega_{nA}^2 - C_{rB}\omega_{nB}^2 + C_{rC}\omega_{nC}^2)}{\text{Den}} \end{cases} \tag{20}$$

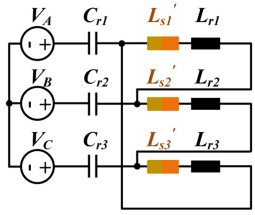

Fig. 25. Short-circuit equivalent circuit of Δ-Cr-Y type topology including stray inductance.

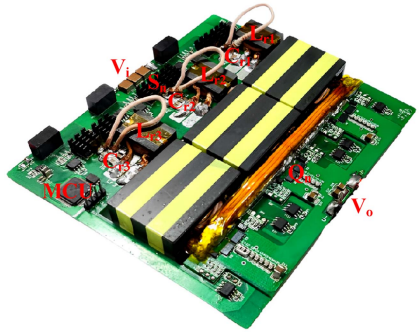

Fig. 26. Prototype of the three-phase interleaved *LLC* converter.

where, $\omega_{nA}/\omega_{nB}/\omega_{nC}$ are three-phase angular frequencies (21), and Den is the denominator of impedance transformation (22)

$$\begin{cases} \omega_{nA} = 2\pi f_{nA} \\ \omega_{nB} = 2\pi f_{nB} \\ \omega_{nC} = 2\pi f_{nC} \end{cases} \tag{21}$$

$$\begin{aligned} \text{Den} = &\left(C_{rA}\omega_{nA}^2 - C_{rB}\omega_{nB}^2\right)^2 + C_{rC}^2\omega_{nC}^4 \\ &- 2C_{rA}C_{rC}\omega_{nA}^2\omega_{nC}^2 - 2C_{rB}C_{rC}\omega_{nB}^2\omega_{nC}^2. \end{aligned} \tag{22}$$

Combining $L_{s1}/L_{s2}/L_{s3}$ and (13)–(22), the equivalent stray inductance per phase $(L'_{s1}/L'_{s2}/L'_{s3})$ can be obtained (23). As shown in Fig. 25 , based on $L'_{s1}/L'_{s2}/L'_{s3}$, the resonant inductance $(L_{r1}/L_{r2}/L_{r3})$ can be adjusted to make the three-phase circuit more balanced

$$\begin{cases} L'_{s1} = \frac{2}{C_{rA}\omega_{nA}^2 + C_{rB}\omega_{nB}^2 - C_{rC}\omega_{nC}^2} - L_{r1} \\ L'_{s2} = \frac{2}{-C_{rA}\omega_{nA}^2 + C_{rB}\omega_{nB}^2 + C_{rC}\omega_{nC}^2} - L_{r2} \\ L'_{s3} = \frac{2}{C_{rA}\omega_{nA}^2 - C_{rB}\omega_{nB}^2 + C_{rC}\omega_{nC}^2} - L_{r3} \end{cases}. \tag{23}$$

Although this method cannot obtain the value of each part of the stray inductance, it can obtain the total stray inductance value of each phase. Combined with the proposed equivalent circuit model, the value of the resonant inductance can be adjusted to make the three-phase circuit more balanced. This article takes the Δ-Cr-Y type three-phase interleaved LLC as an example to demonstrate the resonant inductance adjustment process. Other types of three-phase interleaved *LLC* can also use the proposed optimization method to reduce the influence of stray inductance on current sharing.

IV. Experimental Verifications

To further verify the effectiveness of the proposed method to improve the current sharing performance, a 2-kW prototype

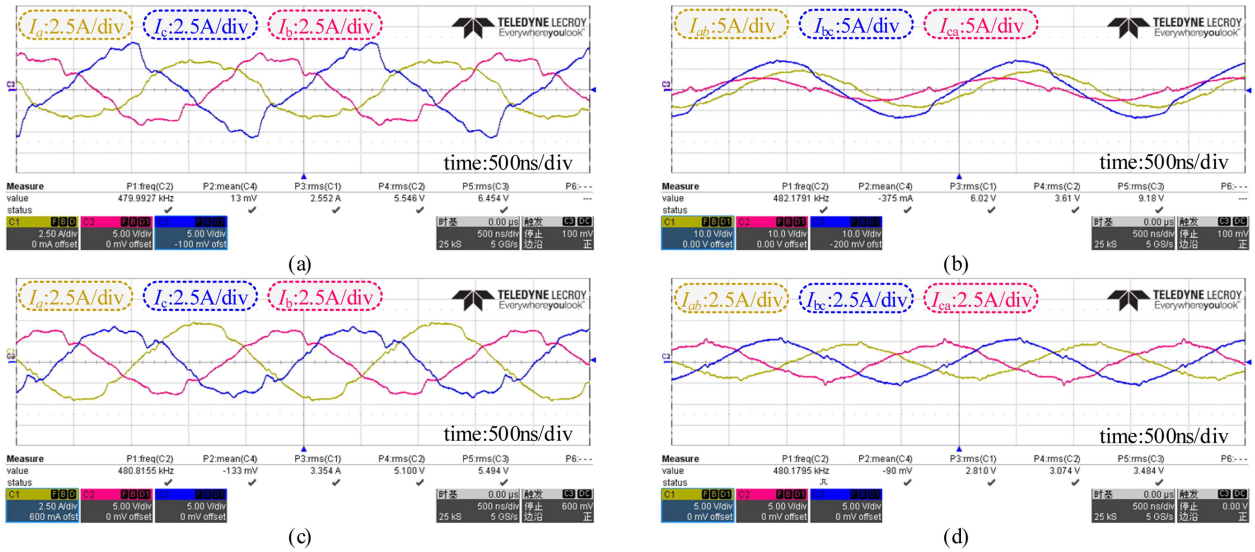

Fig. 27. Current comparison of full-Δ type and Δ-Cr-Y type topologies at half-load. (a) Line current of full-Δ type. (b) Phase current of full-Δ type. (c) Line current of Δ-Cr-Y type. (d) Phase current of Δ-Cr-Y type.

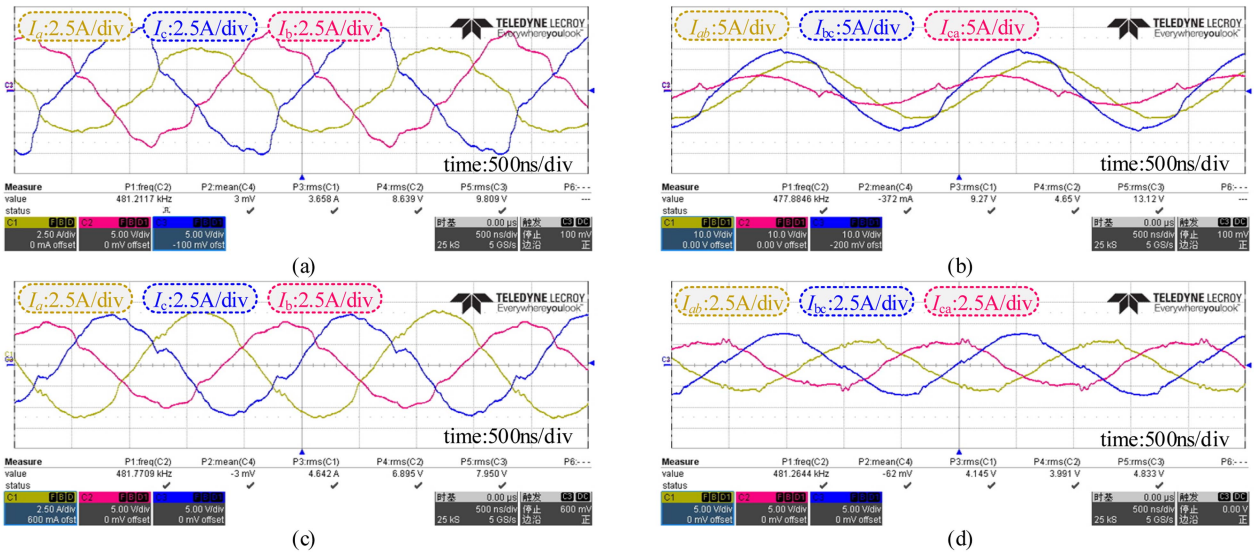

Fig. 28. Current comparison of full-Δ type and Δ-Cr-Y type topologies at full-load. (a) Line current of full-Δ type. (b) Phase current of full-Δ type. (c) Line current of Δ-Cr-Y type. (d) Phase current of Δ-Cr-Y type.

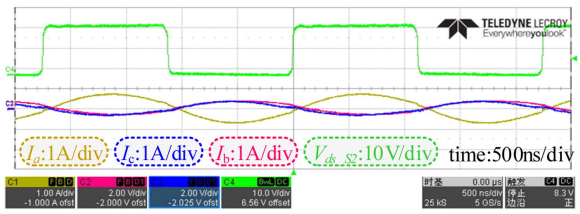

Fig. 29. Key waveforms when f_{sA} is equal to f_{nA}.

is designed in this section (see Fig. 26). Table IV shows the main parameters of the Δ-Cr-Y type, and the parameters of the full-Δ type can be obtained according to the star-delta transformation. The experiment mainly includes two parts: 1) verify that the Δ-Cr-Y topology proposed in Section II can improve the current sharing performance of the full-Δ topology. 2) verify that the optimization method proposed in Section III can further improve the current sharing performance of the Δ-Cr-Y type.

A. Comparison of Current Sharing Performance Between Full-Δ Type and Δ-Cr-Y Type

Fig. 27 shows the line current and phase current of full-Δ topology and Δ-Cr-Y topology at half-load. Fig. 28 shows the line current and phase current of full-Δ topology and Δ-Cr-Y

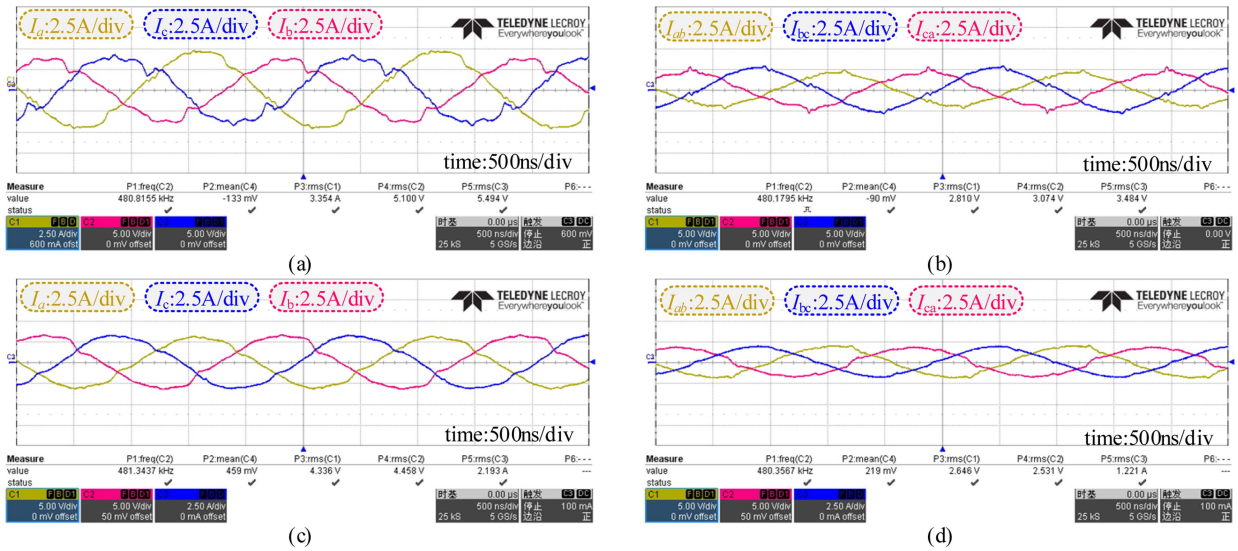

Fig. 30. Current comparison of Δ-Cr-Y topology before and after optimization using the proposed method at half-load. (a) Line current before optimization. (b) Phase current before optimization. (c) Line current after optimization. (d) Phase current after optimization.

TABLE IV
CIRCUIT PARAMETERS OF THE PROTOTYPE

Parameters	Symbol	Value
Input voltage	V_i	400 V
Output voltage	V_o	48 V
Output Power	P_o	2 kW
Magnetizing inductors	L_{m1}, L_{m2}, L_{m3}	≈60 μH
Resonant inductors	L_{r1}, L_{r2}, L_{r3}	≈10 μH
Resonant capacitors	C_{r1}, C_{r2}, C_{r3}	≈27 nF
Magnetic cores	T_1, T_2, T_3	ER41
	L_{r1}, L_{r2}, L_{r3}	EQ20
Primary devices	S_1-S_6	GS66516T
Secondary devices	Q_1-Q_6	EPC2302
Gate drivers	*Dri_p*	Si8271GBD-IS
	Dri_s	1EDB7275FXUMA1
Driver resistors	*DR_p*	5.1 Ω/2 Ω
	DR_s	5.1 Ω/1 Ω
Auxiliary power	-	NEK0509

topology at full-load. It can be seen that there is a large circulating current in the full-Δ type, and the phases of the three-phase phase currents are basically the same, which is consistent with the simulation results. Due to the influence of the circulating current, the peak value of the phase current is larger than the peak value of the line current, which greatly increases the loss. Meanwhile, the line current of the full-Δ type is also imbalanced. In contrast, the Δ-Cr-Y topology has smaller line current and phase current deviations and better current sharing performance. Therefore, changing the resonant capacitor to Y-type connection can improve the current sharing performance of the full-Δ type topology, verifying the theoretical analysis in Section II.

B. Verification of the Proposed Optimization Method to Reduce the Influence of Stray Inductance

Using the proposed optimization method to reduce the influence of stray inductance needs to obtain three resonant frequencies (f_{nA}/f_{nB} /f_{nC}) first. Taking f_{nA} as an example, Fig. 29 shows the waveform when looking for the first resonant frequency according to the short-circuit model. S_3 and S_5 are kept off, S_4 and S_6 are kept ON. Therefore, I_b is almost equal to I_c and half of I_a. When the switching frequency of phase A is equal to f_{nA}, the resonant current I_a has a complete resonant cycle. The three resonant frequencies (f_{nA}/f_{nB}/f_{nC}) needed to calculate the stray inductance in (23) can be obtained based on the same method. In this design, f_{nA}/f_{nB}/f_{nC} are 455/460 /480 kHz, respectively; according to (23), the three-phase stray inductance (L'_{s1}/L'_{s2}/L'_{s3}) can be calculated as 4.8 /1.9 /2.4 μH. L'_{s1} is larger than L'_{s2} and L'_{s3}. According to the measurement, the leakage inductance of the transformer is 3.0/1.0/1.4 μH, respectively. It can be further calculated that the line inductance of each phase is 1.8/0.9/1.0 μH. Therefore, L_{r1}/L_{r2}/L_{r3} can be adjusted to 5.2/8.1/7.6 μH to reduce the deviation of the three-phase equivalent resonant inductance. The reason for the large difference in line inductance and leakage inductance of each phase is that the lengths of the Litz wires used to achieve electrical connections in different phases are different. To facilitate electrical connection when designing the PCB and making the prototype (see Fig. 1), the length of the Litz wire in the Y-type connection is not much different, but the difference is larger in the Δ-type connection. The length of the Litz wire in one phase is longer than the other two phases. Therefore, the line inductance difference and leakage inductance difference between phases are large.

Fig. 30 shows the line current and phase current before and after optimization of the Δ-Cr-Y topology at half-load. Fig. 31 shows the line current and phase current before and after

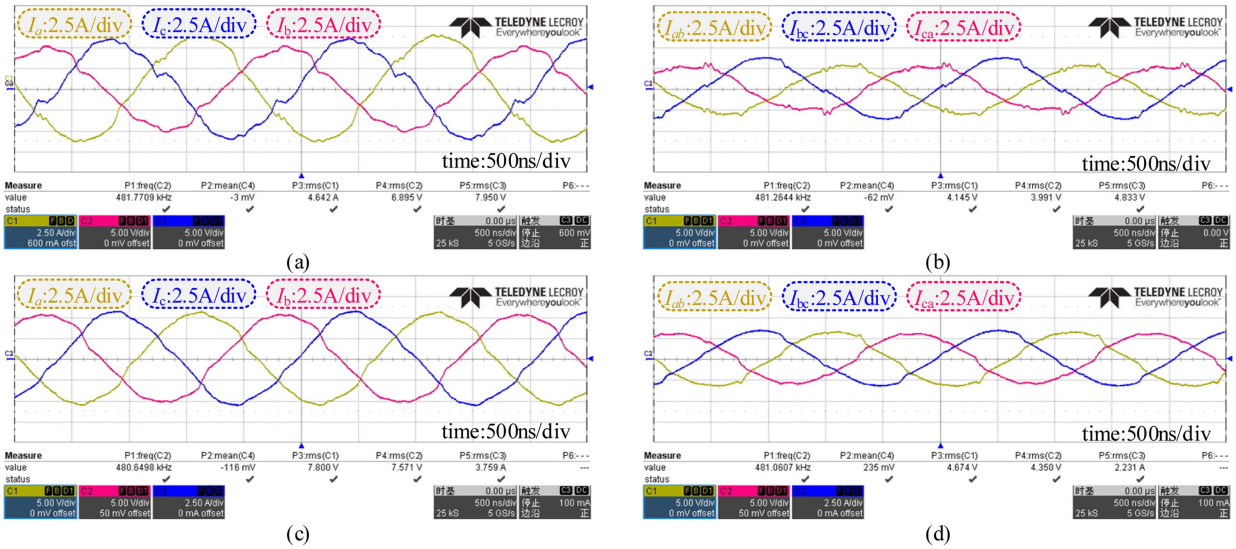

Fig. 31. Current comparison of Δ-Cr-Y topology before and after optimization using the proposed method at full-load. (a) Line current before optimization. (b) Phase current before optimization. (c) Line current after optimization. (d) Phase current after optimization.

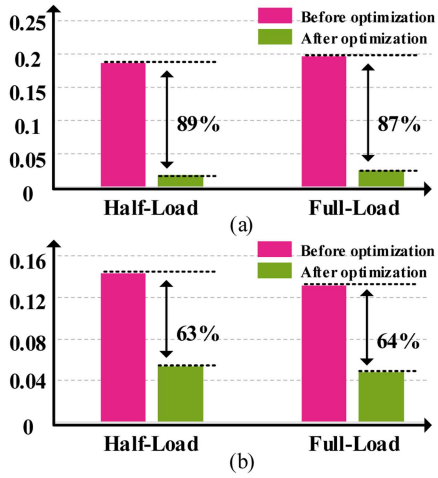

Fig. 32. Comparison of U_f before and after optimization. (a) U_f of line current. (b) U_f of phase current.

optimization of the Δ-Cr-Y topology at full-load. It can be seen that the three-phase current can be more balanced after using the proposed optimization method. Further, Fig. 32 is the comparison of U_f before and after optimization. Using the proposed optimization method can reduce $U_{f\cdot\mathrm{Line}}$ by 89% and $U_{f\cdot\mathrm{Phase}}$ by 63% at half-load. At full-load, after using the proposed optimization method, $U_{f\cdot\mathrm{Line}}$ is reduced by 87%, and $U_{f\cdot\mathrm{Phase}}$ is reduced by 64%. Therefore, the proposed optimization method can greatly reduce the influence of stray inductance on current sharing and make the three-phase current of three-phase interleaved *LLC* more balanced.

Fig. 33 shows the efficiency curves for the three cases. As shown in Fig. 33, the full-Δ type topology has the lowest efficiency due to the severe imbalance of the phase current. In addition, the efficiency of the Δ-Cr-Y type topology was improved by 0.54% using the proposed optimization method.

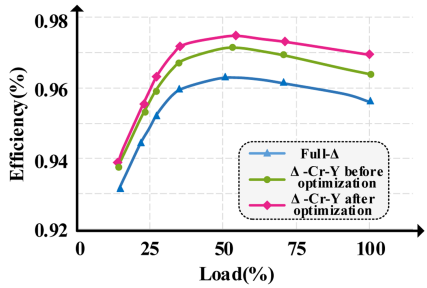

Fig. 33. Efficiency comparison of the three cases.

V. Conclusion

This article proposes a three-power parallel analysis model to compare the current-sharing characteristics of different three-phase interleaved *LLC* topologies. Based on the proposed model, this article finds that although the full-Δ type has lower transformer losses, its current-sharing characteristic is poor. To improve its current-sharing characteristic, a Δ-Cr-Y type three-phase interleaved *LLC* with the same transformer loss was proposed in this article. Further, to reduce the influence of stray inductance on the three-phase current balance, based on the circuit model including stray inductance, this article proposed an optimization method without additional components.

Finally, the theoretical analysis was verified by simulation and experiment. Compared with the full-Δ type, the proposed Δ-Cr-Y type showed higher current balance performance, and the proposed optimization method can further reduce the line current unbalance factor by more than 85%, and the phase current unbalance factor by more than 60%.

References

[1] B. Yang, F. C. Lee, A. J. Zhang, and G. Huang, "LLC resonant converter for front end DC/DC conversion," in *Proc. 17th Annu. IEEE Appl. Power Electron. Conf. Expo.*, 2002, vol. 2, pp. 1108–1112.

[2] S. Luan, Z. Wu, Z. Wang, X. Liu, C. Chen, and Y. Kang, "A high power density two-stage GaN-based isolated Bi-Directional DC-DC converter," in *Proc. IEEE Energy Convers. Congr. Expo.*, 2019, pp. 3240–3244.
[3] Z. Wu, Z. Wang, Y. Zhang, W. Xu, C. Chen, and Y. Kang, "A high efficiency and high power density DC transformer topology with output regulation capability," *IEEE Trans. Power Electron.*, vol. 37, no. 7, pp. 8232–8247, Jul. 2022.
[4] Z. Wang, Z. Wu, T. Liu, C. Chen, and Y. Kang, "A high efficiency and high power density integrated two-stage DC-DC converter based on bipolar symmetric phase shift modulation strategy," *IEEE Trans. Power Electron.*, vol. 37, no. 4, pp. 4358–4373, Apr. 2022.
[5] X. Fang et al., "Efficiency-oriented optimal design of the LLC resonant converter based on peak gain placement," *IEEE Trans. Power Electron.*, vol. 28, no. 5, pp. 2285–2296, May 2013.
[6] Z. Wang, Z. Wu, T. Liu, C. Chen, and Y. Kang, "A high-efficiency and high-power-density interleaved integrated buck-boost-LLC converter and its comprehensive optimal design method," *IEEE Trans. Power Electron.*, vol. 37, no. 9, pp. 10849–10863, Sep. 2022.
[7] J.-E. Yeon, W.-S. Kang, K.-M. Cho, T.-Y. Ahn, and H.-J. Kim, "Multi-phase interleaved LLC-SRC and its digital control scheme," in *Proc. Int. Symp. Power Electron., Elect. Drives, Automat. Motion*, 2010, pp. 1189–1193.
[8] E. Orietti, P. Mattavelli, G. Spiazzi, C. Adragna, and G. Gattavari, "Analysis of multi-phase LLC resonant converters," in *Proc. Braz. Power Electron. Conf.*, 2009, pp. 464–471.
[9] T. Jin and K. Smedley, "Multiphase LLC series resonant converter for microprocessor voltage regulation," in *Proc. Conf. Rec. IEEE Ind. Appl. Conf. 41st IAS Annu. Meeting*, 2006, pp. 2136–2143.
[10] C. Fei, R. Gadelrab, Q. Li, and F. C. Lee, "High-frequency three-phase interleaved LLC resonant converter with GaN devices and integrated planar magnetics," *IEEE J. Emerg. Sel. Topics Power Electron.*, vol. 7, no. 2, pp. 653–663, Jun. 2019.
[11] B. Li, Q. Li, and F. C. Lee, "A WBG based three phase 12.5 kW 500 kHz CLLC resonant converter with integrated PCB winding transformer," in *Proc. IEEE Appl. Power Electron. Conf. Expo.*, 2018, pp. 469–475.
[12] F. Jin, A. Nabih, Q. Li, and F. C. Lee, "A three phase CLLC converter with improved planar integrated transformer for fast charger applications," in *Proc. IEEE 4th Int. Conf. DC Microgrids*, 2021, pp. 1–5.
[13] L. Junkai, Y. Ge, M. Liu, Y. Yang, Q. Wu, and Z. Cheng, "Research on a new control strategy for reducing hard-switching work range of the three-phase interleaved LLC resonant converter," in *Proc. IEEE Int. Telecommun. Energy Conf.*, 2018, pp. 1–6.
[14] A. K. S. Bhat and R. L. Zheng, "A three-phase series-parallel resonant converter-analysis, design, simulation, and experimental results," *IEEE Trans. Ind. Appl.*, vol. 32, no. 4, pp. 951–960, Jul./Aug. 1996.
[15] Y. Nakakohara, H. Otake, T. M. Evans, T. Yoshida, M. Tsuruya, and K. Nakahara, "Three-phase LLC series resonant DC/DC converter using SiC MOSFETs to realize high-voltage and high-frequency operation," *IEEE Trans. Ind. Electron.*, vol. 63, no. 4, pp. 2103–2110, Apr. 2016.
[16] E. Orietti, P. Mattavelli, G. Spiazzi, C. Adragna, and G. Gattavari, "Current sharing in three-phase LLC interleaved resonant converter," in *Proc. IEEE Energy Convers. Congr. Expo.*, 2009, pp. 1145–1152.
[17] S. A. Arshadi, M. Ordonez, W. Eberle, M. A. Saket, M. Craciun, and C. Botting, "Unbalanced three-phase LLC resonant converters: Analysis and trigonometric current balancing," *IEEE Trans. Power Electron.*, vol. 34, no. 3, pp. 2025–2038, Mar. 2019.
[18] S. A. Arshadi, M. Ordonez, and W. Eberle, "Current-sharing worst-case analysis of three-phase CLLC resonant converters," *IEEE Trans. Power Electron.*, vol. 37, no. 3, pp. 3099–3110, Mar. 2022.
[19] M. Noah, J. Imaoka, Y. Ishikura, K. Umetani, and M. Yamamoto, "Review of current balance mechanism in multiphase LLC resonant converters," in *Proc. IEEE 27th Int. Symp. Ind. Electron.*, 2018, pp. 1030–1036.
[20] M. Noah et al., "A current sharing method utilizing single balancing transformer for a multiphase LLC resonant converter with integrated magnetics," *IEEE J. Emerg. Sel. Topics Power Electron.*, vol. 6, no. 2, pp. 977–992, Jun. 2018.
[21] H.-S. Kim, J.-W. Baek, M.-H. Ryu, J.-H. Kim, and J.-H. Jung, "The high-efficiency isolated AC–DC converter using the three-phase interleaved LLC resonant converter employing the Y-connected rectifier," *IEEE Trans. Power Electron.*, vol. 29, no. 8, pp. 4017–4028, Aug. 2014.
[22] H.-S. Kim, J.-W. Baek, and J.-H. Jung, "Output current balancing method for three-phase interleaved LLC resonant converter employing Y-connected rectifier," in *Proc. IEEE Appl. Power Electron. Conf. Expo.*, 2014, pp. 1227–1232.
[23] Z. Hu, Y. Qiu, Y.-F. Liu, and P. C. Sen, "A control strategy and design method for interleaved LLC converters operating at variable switching frequency," *IEEE Trans. Power Electron.*, vol. 29, no. 8, pp. 4426–4437, Aug. 2014.
[24] Z. Hu, Y. Qiu, L. Wang, and Y.-F. Liu, "An interleaved LLC resonant converter operating at constant switching frequency," *IEEE Trans. Power Electron.*, vol. 29, no. 6, pp. 2931–2943, Jun. 2014.
[25] Z. Hu, Y. Qiu, L. Wang, and Y.-F. Liu, "An interleaved LLC resonant converter operating at constant switching frequency," in *Proc. IEEE Energy Convers. Congr. Expo.*, 2012, pp. 3541–3548.
[26] J. Guan et al., "A high efficiency Δ-Lr-Y type three-phase interleaved LLC converter with less transformer loss," *IEEE Trans. Power Electron.*, vol. 38, no. 9, pp. 11152–11168, Sep. 2023, doi: 10.1109/TPEL.2023.3283391.
[27] A. Lordoglu, M. O. Gulbahce, D. A. Kocabas, and S. Dusmez, "Design and optimization of three-phase LLC Charger with Δ – Δ Winding configuration," in *Proc.-48th Annu. Conf. IEEE Ind. Electron. Soc.*, 2022, pp. 1–6.
[28] VISHAY, "Surface mount multilayer ceramic chip capacitors for commercial applications," Mar. 25, 2022. [Online]. Available: https://www.vishay.com/docs/45199/vjcommercialseries.pdf

Jiajia Guan received the B.S. degree in electrical and electronic engineering from the Dalian Maritime University, Dalian, China, in 2020. He is currently working toward the Ph.D. degree in electrical engineering with the School of Electrical and Electronic Engineering, Huazhong University of Science and Technology, Wuhan, China.

His current research interests include high efficiency and high power density converter, magnetic integration and applications of wide bandgap power semiconductor devices.

Jin Wen (Graduate Student Member, IEEE) received the B.S. degree in electrical and electronic engineering in 2021 from the Huazhong University of Science and Technology, Wuhan, China, where he is currently working toward the Master's degree in electrical engineering with the School of Electrical and Electronic Engineering.

His current research interests include high-efficiency and high power density isolated dc–dc conversion and applications of wide bandgap power semiconductor devices.

Shuangxi Zhu (Graduate Student Member, IEEE) received the B.S. degree in electrical engineering and automation, in 2022, from the School of Electrical and Electronic Engineering, Huazhong University of Science and Technology, Wuhan, China, where he is currently working toward the Ph.D. degree in electrical engineering.

His current research interests include high power dc/ac converter and wide bandgap power semiconductor devices packaging.

Zongheng Wu received the B.S. degree in electronic science and technology, in 2017, from the School of Optical and Electronic Information, Huazhong University of Science and Technology, Wuhan, China, where he is currently working toward the Ph.D. degree in electrical engineering with the School of Electrical and Electronic Engineering.

His current research interests include high efficiency and high power density isolated dc–dc conversion and applications of wide bandgap power semiconductor devices.

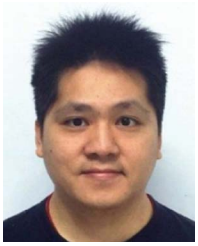

Cai Chen (Member, IEEE) received the B.S. and Ph.D. degrees in electrical and electronic engineering from the Huazhong University of Science and Technology, Wuhan, China, in 2008 and 2014, respectively.

From March 2013 to December 2013, he was an Intern in GE Global Research Center, Shanghai, China. From 2014 to 2016, he was with the Advanced Semiconductor, Packaging and Integration Lab, Huazhong University of Science and Technology, Wuhan, Hubei, China as a Postdoctoral Researcher. From 2016 to 2017, he was a visiting scholar with the Center for High Performance Power Electronics, The Ohio State University, Columbus, OH, USA. From 2017 to 2018, he was a visiting scholar with the College of Engineering, University of Arkansas, Fayetteville, AR, USA. In 2019, he joined the Huazhong University of Science and Technology, Wuhan, China, as an Associate Research Fellow. He is an Associate Research Fellow with the Huazhong University of Science and Technology. His research interests include WBG devices packaging, integration, packaging EMI issues, packaging reliability, and high-density applications.

Yong Kang (Fellow, IEEE) was born in Hubei Province, China, in 1965. He received the B.E., M.E, and Ph.D. degrees in electrical engineering from the Huazhong University of Science and Technology, Wuhan, China, in 1988, 1991, and 1994, respectively.

In 1994, he joined Huazhong University of Science and Technology as a Lecturer and was promoted to Associate professor in 1996 and to Full Professor in 1998. He has authored or coauthored more than 60 technical papers. His research interests include power electronic converter, ac drivers, electromagnetic compatibility, their digital control techniques, and WBG device packaging and applications.